PHYSICAL REVIEW A VOLUME 58, NUMBER 5 NOVEMBER 1998

Observation of an impact-parameter window in low-velocity ionizing collisions of Ne^+ on Ne proceeding through quasimolecular states

M. A. Abdallah,[1,*] W. Wolff,[2] H. E. Wolf,[2] C. L. Cocke,[1] and M. Stöckli[1]
[1]*J.R. Macdonald Laboratory, Kansas State University, Manhattan, Kansas 66506*
[2]*Instituto de Física, Universidade Federal do Rio de Janeiro, Rio de Janeiro, Brazil*
(Received 17 June 1998)

Target ionization in collisions of singly charged Ne^+ ions with Ne has been investigated at projectile velocities from 0.25 to 0.55 a.u. using electron and recoil momentum imaging techniques. The momentum distributions of the ejected electrons were found to carry a distinct signature strongly suggesting that ionization is taking place by successive promotions through molecular orbitals. The observed recoil transverse momentum distributions are donut-shaped, indicating that single ionization is confined to a well-defined impact-parameter window. [S1050-2947(98)50311-3]

PACS number(s): 34.50.Fa, 39.30.+w

Ionization in ion-atom collisions at low to intermediate velocities (0.1 to 1.5 a.u.) has been the subject of extensive experimental and theoretical investigations for many years, and a discussion of earlier results, including a comprehensive list of references, can be found in the recent article of Kravis *et al.* [1]. In particular, the so-called ''saddle-point'' mechanism, originally proposed by Olson [2], has received much attention. It predicted that at low projectile velocities the electron might end up, in momentum space, at a point along the internuclear axis, the ''saddle-point,'' where the forces by the singly charged residual target ion and the receding projectile compensate each other. In the case of a singly charged projectile, this point would correspond to an electron momentum of $V_P/2$, V_P being the projectile velocity. An experimental search for a ''saddle-point'' hump in electron spectra proved elusive, however, with different groups reporting contradictory results.

At much lower projectile velocities, typically 0.05 a.u. and below, molecular promotion was proposed earlier to be the principal mechanism of ionization, and much theoretical as well as experimental effort went into proving it ([3], and references therein). However, this early work could not establish, using the techniques then available, direct evidence to support the proposed molecular mechanism. As of late, this long sought-after direct experimental evidence has started to accumulate by employing momentum imaging techniques [4,5]. The structures recently observed in electron momentum distributions from proton and helium ions on helium are currently interpreted as target ionization preceded by the temporary formation of molecular orbitals between the incident projectile and the target. An electron is promoted during the course of the collision into the continuum by rotational coupling via a series of so-called ''hidden crossings'' of molecular orbitals [6]. Eventually the quasimolecule breaks up due to the receding projectile, and the electron is left ''stranded,'' its final momentum distribution carrying a distinct signature of the molecular orbital (MO) it has occupied previous to rupture.

*Present address: Physics Division, ORNL, Oak Ridge, TN 37831-6377. Electronic address: abdallah@mail.phy.ornl.gov

The experimental technique, referred to as COLTRIMS (cold target recoil ion momentum spectroscopy) in the literature, that has made possible these insights into the mechanisms of low-velocity ionization has been described in some detail in [5,7]. The present experiment was carried out at the J.R. Macdonald Laboratory at Kansas State University. The target was a cold, supersonic Ne gas jet, intersected perpendicularly by the projectile beam. Electrons and target recoil ions were extracted from the collision region by an electric field applied perpendicular to the both the incident beam and the gas jet, and detected in coincidence by position-sensitive channel-plate detectors.

For the purpose of data analysis, the same coordinate system as that used in Refs. [5,4] was adopted: The incident beam defines the Z axis, the X axis is perpendicular to the (parallel) planes of the electron and recoil detectors and parallel to the extraction electric field, and the Y axis coincides with the axis of the target gas jet. The Y and Z components of both recoil and electron momentum were directly derived from the impact positions on the respective detectors. The recoil momentum's X component was determined from the recoil's flight time, while the X component of the electron momentum remained undetermined, since the electron signal served as start signal for measuring the recoil's time of flight. The determination of all three components of the recoil momentum was crucial in the present context, since it allowed the selection of scattering planes and impact-parameter windows as well as the separation of single from double ionization events. The latter separation was accomplished by admitting only those events for data analysis that corresponded to certain ranges of the Z component of the recoil momentum (henceforth called the longitudinal component, or $P_{r\|}$), which is directly related to the Q value of the reaction involved.

The singling-out of a scattering plane, defined by the Z axis (the incident beam) and the direction of the emitted recoil, was done by the selection of ranges of the transverse recoil momentum. We have generated distributions of the electron's P_{eY} and P_{eZ} momentum components for two special recoil planes, the XZ plane, which lies perpendicular to the electron detector plane, and the YZ plane, parallel to the electron detector. The former plane produced a ''sideview''

distribution; that is, the projection of the electron momentum distribution onto a plane (the detector plane) perpendicular to the scattering plane. The latter plane produced a ''top-view'' distribution, which is the projection of the electron momentum distribution onto the scattering plane. As a first step towards the selection of these two views, the recoil transverse momentum $P_{r\perp}$ (P_{rX},P_{rY}) distribution was generated from the data. In a second step, gates were placed on this distribution. One gate (G1) selected recoils with small values of P_{rX}, i.e., recoils, which were essentially emitted in the YZ plane and consequently produced ''topview'' electron momentum distributions. A second gate (G2) selected recoils with a small P_{rY}, that is, recoils emitted in the XZ plane, and produced ''side-view'' electron momentum distributions.

In the present article we concentrate on recoil as well as electron momentum distributions obtained for Ne^+ ions colliding with Ne at projectile velocities of 0.25, 0.35, 0.45, and 0.55 a.u. Figures 1(a)–1(d) show the recoil $(P_{rY},P_{r\|})$ momentum distributions for all projectile velocities. Note that the values of $P_{r\|}$ have been converted into Q values using the standard relation $Q=-V_P(P_{r\|}+P_{e\|})$, where $P_{e\|}$ stands for the electron momentum component parallel to the beam (longitudinal component). The small, low-intensity feature visible close to $(P_{rY},P_{r\|})=0$ consists of random coincident events due to resonant electron capture to the ground state. Two distinguished features are visible in these distributions. The first can be identified by its Q value to be due to single ionization events. The second feature, well separated from single ionization by its larger Q value, is associated with simultaneous single ionization and excitation and with target and projectile ionization. Gates were placed on these spectra in order to select a range of Q values corresponding to single ionization events only. Figures 1(e)–1(h) give the recoil transverse momentum $(P_{r\perp})$ distributions corresponding to those gates. The appearance of donuts in these distributions, except at the highest velocity, points to the existence of well-defined impact-parameter windows in the ionizing collisions studied here.

In Figs. 2(a)–2(d) we show top-view electron momentum distributions corresponding to the G1 gates, whose associated $P_{r\perp}$ values are given in the figure caption. The horizontal dashed line in each of these figures marks $P_{eY}=0$ (the beam axis), while the two vertical dashed lines mark $P_{eZ}=0$ and $P_{eZ}=V_P$ (the target and projectile ''position,'' respectively). Note that all horizontal and vertical scales are given in units of V_P (where atomic units are used) to ease comparison. In these distributions the recoil is emitted vertically upward along the $P_{eZ}=0$ line. Side-view distributions, not shown, showed only that the electrons are highly concentrated in the collision plane, a fact that allows producing meaningful top views from the experiment with only two of the three electron momentum components known.

The first three top-view distributions, Figs. 2(a)–2(c), generated by gates G1 on the respective donuts, strikingly resemble the shape of the letter S or that of a spiral galaxy, consisting of two widely open branches or arms connected at the center line through a short and narrow ridge. A noteworthy property of the two branches, most prominent at the lowest velocity, is that they are flung out beyond $P_{eZ}=0$ (the upper branch) and $P_{eZ}=V_P$ (the lower branch). As one goes

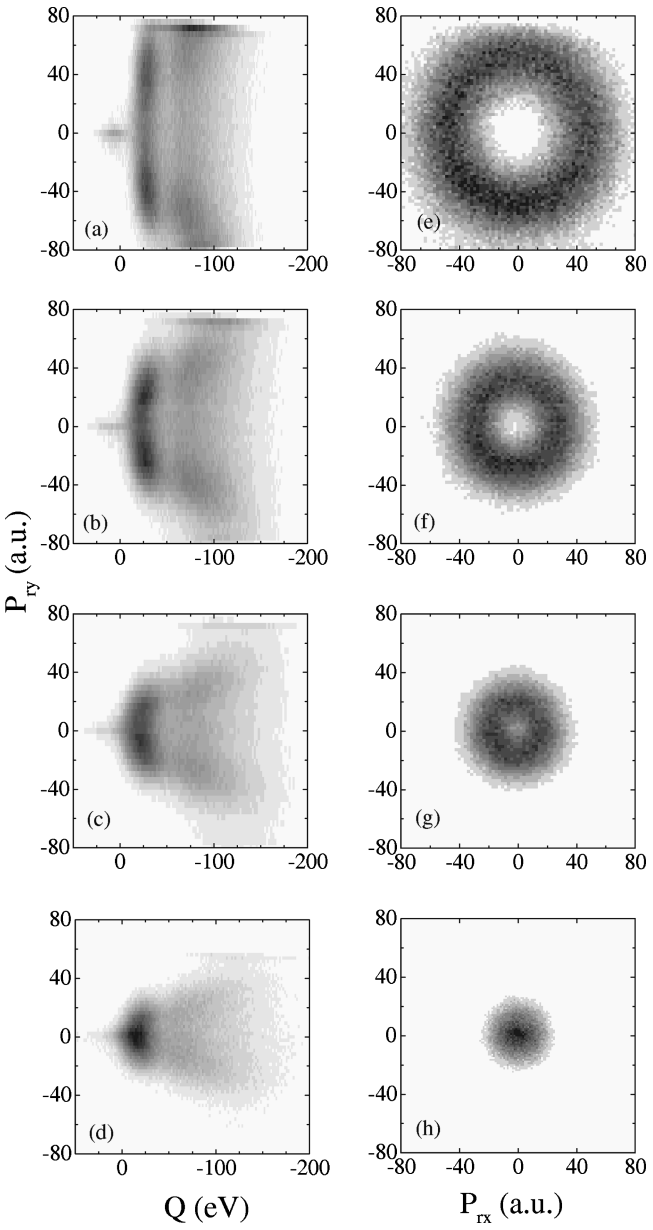

FIG. 1. Recoil momentum distributions from ionizing collisions from Ne^+ incident on Ne for projectile velocities of (from top to bottom) 0.25, 0.35, 0.45, and 0.55 a.u. The first column of figures [(a)–(d)] shows P_{rY}, one of the transverse momentum components, versus the longitudinal momentum $P_{r\|}$ transformed into Q values, while the second column of figures [(e)–(h)] shows the recoil transverse momentum distributions.

from lower to higher projectile velocities the S shape appears to rotate into a more upright position, the upper branch gains in intensity compared to the lower branch, and the whole electron distribution becomes increasingly more confined inside the ''velocity window'' defined by $P_{eZ}=0$ and $P_{eZ}=V_P$.

Another interesting fact about these topview electron distributions is the presence of a ridge sitting on the beam axis, while the opposite, a valley or nodal line, has been observed previously in the (H^+, He^+)-He systems. A more detailed view of this ridge can be gained by projecting thin slices cut out of the top-view electron distributions along and across (at $P_{eZ}=V_P/2$) the $P_{eY}=0$ line onto the P_{eZ} and the P_{eY} axis

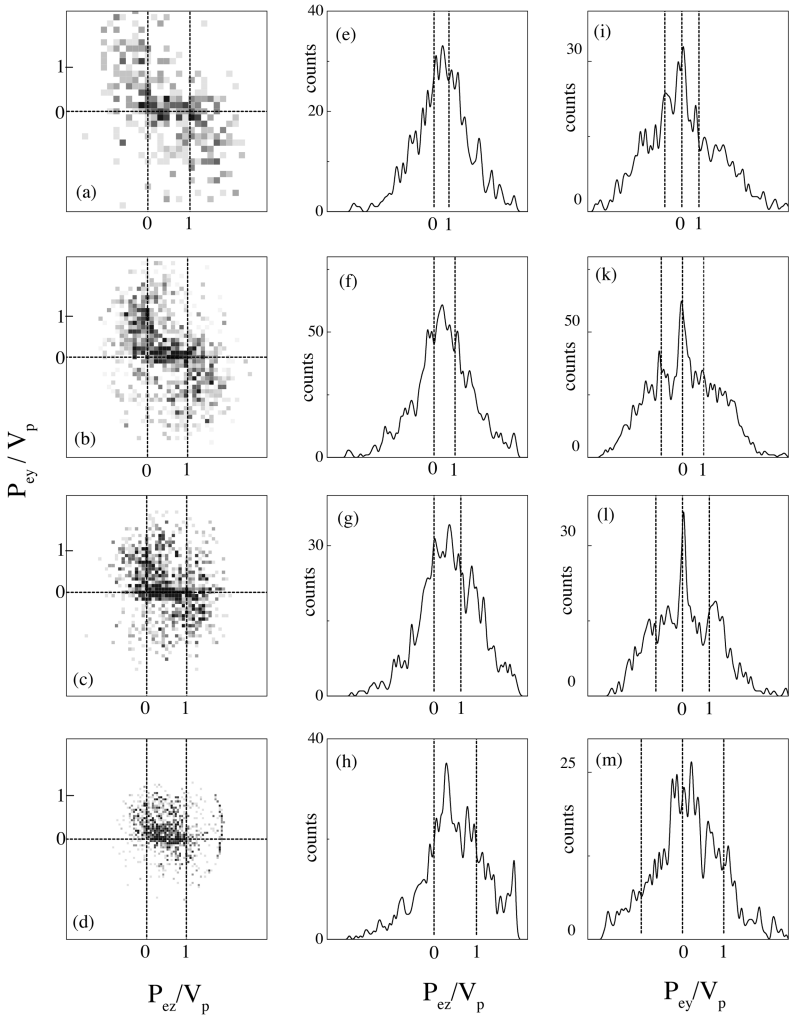

FIG. 2. ''Top view'' (in-plane) electron momentum distributions, proceeding from the top row to the bottom one, for $V_P=0.25$, 0.35, 0.45 and 0.55 a.u. (a)–(d) as well as thin slices cut out of these distributions along (e)–(h) and across (i)–(m), the beam axis (the horizontal dashed line), and projected onto the horizontal and vertical axis, respectively. Both horizontal and vertical axes of the topviews are given in units of V_P (where atomic units are used). The top views correspond to recoil transverse momentum windows centered around $P_{r\perp}=48$ a.u. for $V_P=0.25$ a.u., 26.5 a.u. for $V_P=0.35$ a.u, 15 a.u. for $V_P=0.45$ a.u, and 8 a.u. for $V_P=0.55$ a.u. and $P_{r\|}$ centered on single ionization.

(''horizontal'' and ''vertical'' slices). This is done in Figs. 2(e)–2(h) and Figs. 2(i)–2(m), respectively. In the horizontal slices the ridge appears as a broad distribution roughly centered around $P_{eZ}=V_P/2$. The vertical slices reveal that from 0.25 to 0.45 a.u. the ridge is a very narrow, spikelike feature, most prominent at 0.45 a.u. Lateral structures are caused by the branches intruding into these vertical slices.

At 0.55 a.u., a different picture begins to emerge. The lower branch has almost disappeared and the upper branch has lost intensity as well and appears more curved. Electrons are now seen to concentrate in a broad feature, occupying the space between $P_{eZ}=0$ and $P_{eZ}=V_P$ and being displaced from the center line into the upper half of the scattering plane. In fact, most of the electron distribution is now located in the upper half of that plane. The vertical slice reflects this new feature. The ridge observed at lower velocities has given way to a broader distribution centered around $P_{eY}=0$.

It is instructive to compare the results obtained for three collision systems investigated to date, H^+ and He^+ on He and Ne^+ on Ne. The two-finger or double-wing feature observed in the top-view electron distributions in H^+ and He^+ on He is replaced in the Ne case by two spiral arms emanating from the target and the projectile ''position'' into opposite directions. Qualitatively these features are very similar and are presumably of the same origin; i.e., carry the signature of the final molecular orbit the electron occupied prior to rupture of the dynamic quasimolecule. For the purpose of comparison, we show side by side in Figs. 3(a) and 3(b) the 0.45-a.u. Ne^+-Ne electron top-view distribution and a selected (around $P_{r\perp}=7$ a.u.) top-view distribution from He^+-He, at $V_P=0.9$ a.u. The similarity between the wings in He^+-He and the spiral arms in Ne^+-Ne is obvious. However, the orientation of the branches appears reversed. In the Ne^+-Ne case the branch anchored at the target position points upwards, while its counterpart in the He^+-He system points downwards. The opposite holds true for the projectile-anchored branches. In addition, the He^+-He double-wing feature is confined, in velocity space, between target and projectile, while the Ne^+-Ne branches are much wider, extending beyond both target ($P_{eZ}<0$) and projectile ($P_{eZ}>V_P$).

Another qualitative difference between the two distributions of Figs. 3(a) and 3(b) is the presence of a central ridge in Ne^+-Ne as opposed to a nodal line in He^+-He. This can be seen more clearly by comparing projected slices, Figs. 3(c)–3(f). The ''horizontal'' slice from He^+-He [Fig. 3(d)] reveals the presence of higher intensity both close to the target and the projectile, while the ''vertical'' slice [Fig. 3(f)] shows the accentuated nodal line between the two branches. Conceivably the central ridge occupying the momentum

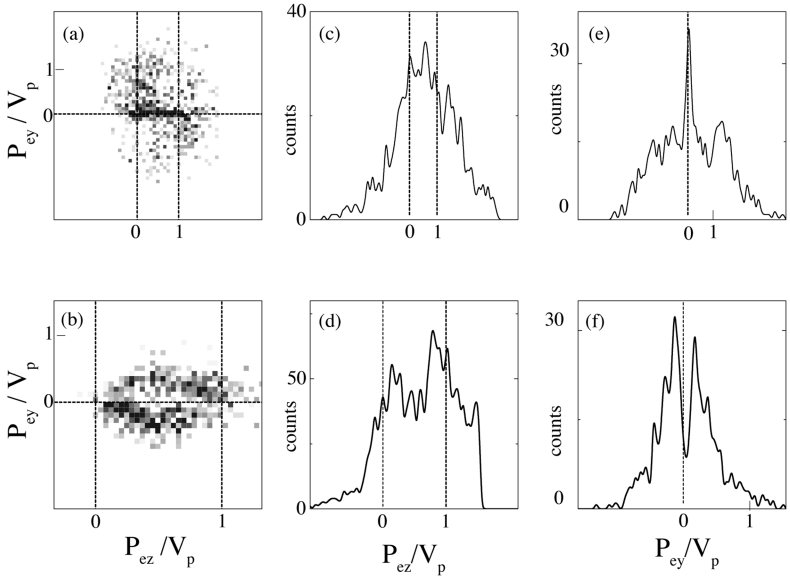

FIG. 3. ''Top-view'' electron momentum distributions from (a) Ne^+ on Ne at $V_P=0.45$ a.u. and $P_{r\perp}=15$ a.u. and (b) He^+ on He at $V_P=0.9$ a.u. and $P_{r\perp}=7$ a.u. As in Fig. 2 thin slices were cut out of these distributions along (c), (d) and across (e), (f) the beam axis, and projected onto the horizontal and vertical axes, respectively.

space between target and projectile in Ne^+-Ne also carries the signature of a promoted molecular orbital.

A final remarkable distinction between the collision systems consists in the appearance of a donut in the recoil transverse momentum distributions in Ne^+-Ne. The donuts signal that single target ionization is taking place within a narrow range of impact parameters. From the donut radii, reduced scattering angles were extracted whose values were found to be close to those reported by [3], suggesting the existence of a ''critical promotion radius,'' probably related to the $4f\sigma_u$ MO . A possible explanation for the existence of an impact-parameter window for Ne^+ on Ne, which was absent for p and He ions on He, can be found in the calculations of Brenot *et al.* [3]. The molecular orbital which is a likely candidate for promoting an electron into the continuum, $4f\sigma_u$, exhibits a steep slope with decreasing internuclear separation R. In addition, their calculations revealed a tight bunching of potential-energy curves and crossings within a narrow range of R, at around 1.6 a.u., out of which the steeply rising $4f\sigma_u$ MO emerges. This then would be the cause of the well-defined upper limit (the inner radius of the transverse recoil momentum donut) for the impact parameter leading to ionization through molecular promotion. The lower limit (the donut's outer radius) is caused by the onset of target and projectile excitation and/or double ionization, a fact that was already apparent from the recoil $(P_{rY},P_{r\|})$ distributions of Figs. 1(a)–1(d).

In conclusion we have presented results from Ne^+ colliding with Ne, exhibiting different features and thus providing a timely contribution to augment our still incomplete knowledge about low-velocity ionization processes. The electron momentum images presented here show clear qualitative differences between ionizing cases where (a) π-structure from rotational coupling and (b) σ-structure where radial coupling is likely to dominate. The former has no impact parameter threshold, while the latter does, as evident from the donuts presently observed in the recoil transverse momentum distributions. We attribute this behavior to $4f\sigma_u$ MO promotion. Furthermore, the electron momentum spectra seen for this case, presmuably displaying signatures of the promoted orbital, differ dramatically from those seen previously in rotational-coupling-dominated cases.

This work was supported by the Division of Chemical Sciences, Office of Basic Energy Sciences, Office of Energy Research and the U.S. Department of Energy.

[1] S.D. Kravis, M. Abdallah, C.L. Cocke, C.D. Lin, M. Stöckli, B. Walch, Y.D. Wang, R.E. Olson, V.D. Rodriguez, W. Wu, M. Pieksma, and N. Watanabe, Phys. Rev. A **54**, 1394 (1996).

[2] R.E. Olson, Phys. Rev. A **27**, 1871 (1983).

[3] J.C. Brenot, D. Dhuicq, J.P. Gauyacq, J. Pommier, V. Sidis, M. Barat, and E. Pollack, Phys. Rev. A **11**, 1245 (1975).

[4] R. Dörner, H. Khemliche, M.H. Prior, C.L. Cocke, J.A. Gary, R.E. Olson, V. Mergel, J. Ullrich, and H. Schmidt-Böcking, Phys. Rev. Lett. **77**, 4520 (1996).

[5] M.A. Abdallah, C.L. Cocke, W. Wolff, H. Wolf, S.D. Kravis, M. Stöckli, and E. Kamber (unpublished).

[6] J.H. Macek and S. Yu Ovchinnikov, Phys. Rev. Lett. **80**, 2298 (1998).

[7] J. Ullrich, R. Moshammer, R. Dörner, O. Jagutzki, V. Mergel, H. Schmidt-Böcking, and L. Spielberger, J. Phys. B **30**, 2917 (1997).